The Size of Turbulent Eddies Close to a Wall

Coherent flow-oriented structures, with a dimensionless spacing of $\lambda^+ \approx 100$, observed close to a wall in turbulent flows are believed to control the production of turbulence. A 2½ D computer model developed by Nikolaides is used to explain the dimensionless spacing of these structures. The calculations suggest that the net production of turbulence in the viscous wall region is sensitive to changes in λ^+ in the neighborhood of $\lambda^+ \approx 100$. They indicate that the net production is negative for $\lambda^+ < 85$ and that for $\lambda^+ = 93$ the net production is large enough to supply the turbulent energy dissipated in the outer flow.

Stephen L. Lyons,
Christos Nikolaides,
Thomas J. Hanratty
Department of Chemical Engineering
University of Illinois
Urbana, IL 61801

Introduction

The viscous wall layer of a turbulent flow is the region close to the wall where viscosity makes a significant direct contribution to the transfer of momentum. It occupies the space between $y^+ = 0$ and $y^+ = 30$–40, where y^+ is the distance from the wall made dimensionless using the wall parameters, ν and $u^* = (\tau_w/\rho)^{1/2}$. In recent years considerable attention has been given to the discovery that turbulent flow in the viscous wall layer is coherent and that repetitive processes can be identified that seem to control the production of turbulence and the level of Reynolds stress.

These structures were first observed by Beatty et al., (Corrsin 1956) who pumped dye solution through a pipe and, after flushing with water, observed the formation of the residual dye into streamwise filaments at the wall. Kline and his coworkers (Kline and Runstadler 1959; Kim et al., 1971; Kline et al., 1967) through the extensive utilization of these dye techniques, as well as hydrogen bubble techniques, properly interpreted these results. They showed that the wall dye streaks are regions of low axial velocities and that, after lifting from the wall, the streaks undergo a strong interaction, called a burst, with the turbulent fluid outside the viscous wall region. A number of laboratories have confirmed these results and have added additional qualitative and quantitative information about the kinematics of the viscous wall layer. In particular, the early experiments of Corino and Brodkey (1969) should be mentioned. The two chief parameters that have resulted from these studies are the spacing between streaks, λ_1, and the period between bursts, T_B.

The importance of these parameters is emphasized by the findings that polymer drag-reduction is associated with an increase in $\lambda_1^+ = \lambda_1^* u/\nu$ (Fortuna and Hanratty, 1972; Eckelman et al. (1972) and that the decrease of drag in the presence of a favorable pressure gradient is associated with an increase in both λ_1^+ and $T_B^+ = T_B u^{*2}/\nu$.

This paper examines the question of why $\lambda_1^+ \simeq 100$ for the turbulent flow of a Newtonian fluid in a low-pressure gradient. This is accomplished by using the 2½ D models for the viscous wall layer recently explored by Hatziavramidis and Hanratty (1979), Chapman and Kuhn (1981), and Nikolaides (1984).

These models use the observation that important aspects of the flow close to a wall are associated with flow structures elongated in the flow direction. The approach taken is to solve the unaveraged Navier-Stokes equations in the region $0 < y^+ < y_0^+$, using appropriate time-varying boundary conditions at the edge of the viscous wall region, y_0^+. The solution is greatly simplified by neglecting terms containing the variation of hydrodynamic quantities in the flow direction. In this way the y and z momentum equations are decoupled from the streamwise momentum equation, and the three components of the velocity vector are calculated only in planes perpendicular to the x axis.

Hatziavramidis and Hanratty (H-H; 1979) represented the spanwise flow at y_0^+ as being periodic in the spanwise direction and periodic in time, $w = w_L \sin(2\pi z/\lambda_1) \cos(2\pi t/T_B)$, where λ_1 is the spacing of the wall structures, T_B is the period between bursts, and w_L is a constant whose value is consistent with turbulence measurements at y_0. The properties of the calculated periodic flow field were averaged in z and in t for fixed values of y. Good agreement was obtained with measured statistical properties of the turbulence, particularly for $y^+ < 15$. The chief failings of the analysis were that it did not give the correct variation of the normal and spanwise velocity fluctuations with distance from the wall and that it gave an unreasonable picture of the turbulent energy balance for $y^+ > 15$.

Nikolaides (1984) pointed out a number of physical features of the H-H model that are at variance with measurements at $y^+ > 20$: The correlation measurements of Grant (1958) and Tritton (1967) and the frequency-wave number spectra of Mor-

Correspondence concerning this paper should be addressed to Thomas J. Hanratty at the University of Illinois.

rison and Kronauer (1969) reveal that at $y^+ \approx 40$ the most energetic spanwise and streamwise fluctuations are characterized by spanwise wavelengths larger than $\lambda^+ = 100$. Recent conditionally averaged measurements (Nikolaides et al., 1983) relating the pattern of the spanwise component of the wall velocity gradient, s_z, to spanwise velocity fluctuations at different y^+ indicate that, on average, the streamline pattern in a plane perpendicular to the flow is closed rather than open, as suggested by the H-H model; Figure 1.

These contradictory results prompted Nikolaides (1984) to repeat the H-H calculations using more realistic boundary conditions at y_0^+. A number of possibilities were explored, including a randomly varying outer velocity field. It was found that the simplest model that gives results consistent with experiments is one for which the flow at y_0^+ is periodic in space and time, and is characterized by two length scales, $\lambda_1^+ = 100$ and $\lambda_2^+ = 400$. The results of this computer simulation gave good agreement with measurements of statistical characteristics of the turbulence for $0 < y^+ < 30$: the intensities of the three components of turbulent velocity fluctuations, the Reynolds stress, the skewness and flatness of the streamwise velocity fluctuations, the quadrant analysis of the Reynolds stress, and the terms in the turbulent energy balance. The results agree with the conclusions of H-H that $\lambda_1^+ = 100$ eddies are controlling the production of streamwise velocity fluctuations and are a principal contributor to the Reynolds stresses in the viscous wall region. Furthermore, Nikolaides' calculations show intermittent appearances of pairs of $\lambda_1^+ = 100$ stress producing eddies and of isolated wall eddies of smaller size, which seem consistent with experimental observations (Lee et al., 1974; Nikolaides et al., 1983).

The success of the computer model of H-H, as modified by Nikolaides, prompted us to use it to explore why $\lambda_1^+ \approx 100$. The approach taken was simply to carry out calculations of the flow in the viscous wall region for different λ_1^+. However, it should be recognized that the flow characteristics depend not only on the scaling of λ_1, but also on the thickness of the viscous wall region y_0, the magnitude of the velocity fluctuations q, and the time scale of the velocity fluctuations T. Consequently, a critical problem in this study, to be dealt with in the section below on scaling, was the determination of how y_0^+ should vary with λ_1^+.

Main Thrust

The computer solutions of Nikolaides are a model in that they do not pretend to represent exactly the behavior of the viscous wall layer. Rather, they explore whether one can substitute for the exact behavior a periodically varying velocity field which has average properties similar to laboratory measurements. The principal physical question asked is what is the simplest set of boundary conditions at y_0^+ that represent available laboratory measurements?

Although the calculations simplify the equations of motion by assuming homogeneity in the flow direction, the resulting time-varying velocity field can be used to construct a flow field that is varying in the flow direction, x. This is done by using Taylor's hypothesis and multiplying the time variable with a convection velocity U_c^+, which can be taken as approximately equal to 15 for the viscous wall layer. By doing this, small-scale motions in the flow direction are captured. However, it cannot be expected that the model calculations represent all of the small-scale phenomena that have been observed in the laboratory. In this sense the ideas presented by Nikolaides are provocative and their usefulness will be judged by the extent to which they provide an understanding of the physics of wall turbulence.

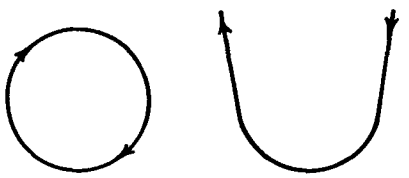

Figure 1. Percentage of closed flow.

The model is really an extension of ideas presented by Townsend (1976) in his pioneering book on the structure of turbulent shear flow. Townsend describes the log layer as being dominated by attached wall eddies (elongated in the flow direction) that increase in size linearly with distance from the wall. The computer experiments take the viewpoint that it is advantageous to consider the viscous wall layer and the outer flow separately. In fact their principal focus is the interaction between the inner and outer layers. The smallest of these "Townsend eddies" has a dimension of $\lambda_1^+ = 100$ and controls the production of turbulence. These $\lambda_1^+ = 100$ eddies bring high-momentum fluid to the wall where they exchange momentum with the wall to create streamwise velocity fluctuations. These streamwise fluctuations are converted to normal and spanwise fluctuations in the outer flow through pressure-velocity correlations.

A feature in this approach is the recognition that the viscous wall region is the engine that drives wall turbulence, since a net production of turbulence occurs there and dissipation is equal to or dominates production in the entire outer region. The main thrust of the present paper is the exploration of an interesting feedback between the inner and outer flows which controls the size of the eddies. This is based on the finding that the net production in the viscous wall region increases monotonically with λ_1^+ and on the expectation that dissipation in the outer flow decreases with increasing λ_1^+.

Scaling

The outer edge of the viscous wall layer, y_0, lies in a region where the mean velocity U varies with the logarithm of the distance from the wall and the velocity gradient is given by the equation

$$\frac{d\bar{U}}{dy} = \frac{u^*}{\kappa y} \tag{1}$$

where $\kappa = 0.41$ is the von Karman constant.

An established property of the log layer is that the production of turbulent energy, $-\overline{uv}\, d\bar{U}/dy$, is approximately equal to the rate of dissipation of turbulent energy, designated as ϵ [Townsend, 1976, p. 138; Hinze, 1975, pp. 649, 737; Bradshaw, 1976, p. 36). Therefore, since y_0 is assumed to be at the inner edge of the log layer,

$$\left(-\overline{uv}\frac{d\bar{U}}{dy}\right)_{y=y_0} \simeq [\epsilon]_{y=y_0}. \tag{2}$$

Outside the viscous wall layer an inviscid estimate can be made for the dissipation which Tennekes and Lumley (1977, p.

21) call "one of the cornerstone assumptions of turbulence theory":

$$\epsilon = a_1 \frac{q^3}{\ell} \tag{3}$$

where $q^2 = \overline{u^2} + \overline{v^2} + \overline{w^2}$ and ℓ is a characteristic length of the large eddies. In applying Eq. 3 to wall turbulence it follows that, in the log layer ℓ varies linearly with distance from the wall and equals the Prandtl mixing length (Bradshaw, 1976, p. 37). This can be seen by substituting Eq. 1 into Eq. 2. The resulting equation is satisfied at $y = y_0$ if

$$\ell = \kappa y_0 \tag{4}$$

and

$$q_0 = \left(\frac{1}{a_1}\right)^{1/3} u^* \tag{5}$$

The picture presented for the organized wall eddy by Nikolaides suggests that its characteristic length in the spanwise direction, λ_1, is related to the distance in the z direction between zero crossings of the v velocity at y_0. For a Gaussian signal the zero crossing scale, defined as $\Lambda = \frac{1}{2}\pi N_0$ (where N_0 is the frequency of the signal) is equal to the Taylor microscale, λ_g (Rice, 1954). The probability distribution for u velocity fluctuations shows a significant departure from a Gaussian behavior at y_0. This is not the case for the v and w velocities. Measurements by Barlow and Johnston (1985) give a skewness of zero and a flatness of three for these velocity components for $y^+ > 30$. Consequently, Nikolaides assumed the wavelength of the wall eddies scales with the Taylor microscale at $y = y_0$; i.e.,

$$\lambda_g|_{y_0} \simeq \lambda_1/2\pi \tag{6}$$

For an isotropic turbulence (Hinze, 1975, p. 219)

$$\epsilon = 15\nu \frac{\overline{u^2}}{\lambda_g^2} \tag{7}$$

This equation has also been used to define the Taylor microscale in anisotropic turbulence with $3\overline{u^2} = (\overline{u_1^2} + \overline{u_2^2} + \overline{u_3^2}) = q^2$ (Tennekes and Lumley, 1972, p. 66). By equating Eqs. 7 and 3, and substituting Eq. 6 for λ_g, it is found that

$$\lambda_1^{+2} = C_5\, y_0^+ \tag{8}$$

with $C_5 \simeq 20\kappa\,\pi^2/a_1^{2/3} \approx 750$. Equation 8 gives $\lambda_1^+ \approx 170$ if $y_0^+ = 40$ and $\lambda_1^+ \approx 150$ if $y_0^+ = 30$, in rough agreement with the value of $\lambda_1^+ = 100$ observed for the streak spacing at the wall. Equation 8 is the same as the relations derived on page 225 of Hinze (1975) and on page 67 of Tennekes and Lumley (1972), if κy_0 is substituted for ℓ. The justification usually adopted for applying Eq. 7 to shear flows is the assumption that small-scale eddies defining λ_g are isotropic, even though the large-scale turbulence is anisotropic. Errors in this assumption are not critical since Eq. 7 is used here only to obtain a scaling relation, and not to predict a value for λ_1.

Nikolaides 2½ D Model

Defining equations and boundary conditions

The continuum equations that describe the flow field are the time-dependent Navier-Stokes equations, for a flow homogeneous in the x direction, and the equation of conservation of mass:

$$\frac{\partial v}{\partial t} + \frac{\partial}{\partial y}(v^2) + \frac{\partial}{\partial z}(vw) = -\frac{\partial p}{\partial y} + \frac{1}{Re}\left(\frac{\partial^2 v}{\partial y^2} + \frac{\partial^2 v}{dz^2}\right) \tag{9}$$

$$\frac{\partial w}{\partial t} + \frac{\partial}{\partial y}(vw) + \frac{\partial}{\partial z}(w^2) = -\frac{\partial p}{\partial z} + \frac{1}{Re}\left(\frac{\partial^2 w}{\partial y^2} + \frac{\partial^2 w}{\partial z^2}\right) \tag{10}$$

$$\frac{\partial U}{\partial t} + \frac{\partial}{\partial y}(vU) + \frac{\partial}{\partial z}(wU) = \frac{1}{Re}\left(\frac{\partial^2 U}{\partial y^2} + \frac{\partial^2 U}{\partial z^2}\right) \tag{11}$$

$$\frac{\partial w}{\partial z} + \frac{\partial v}{\partial y} = 0 \tag{12}$$

All variables are dimensionless with respect to a characteristic length λ_1, and a characteristic velocity equal to twice the root mean square value of the normal velocity fluctuations at y_0. Thus $Re = \lambda_1\, 2\,(\overline{v^2})^{1/2}_{\text{at}\,y_0}/\nu = 182$.

The boundary conditions used at the wall and at the sides of the computational domain are the no-slip conditions and the symmetry conditions:

$$U = v = w = 0 \quad \text{at } y = 0$$

$$w = 0, \frac{\partial v}{\partial z} = 0, \frac{\partial U}{\partial z} = 0 \quad \text{at} \begin{cases} z = 0 \\ z = z_0 \end{cases}$$

where $z_0 = \lambda_2/2$ and λ_2 is the (dimensionless) wavelength of the outer flow eddies. At the upper boundary, y_0, the following conditions are prescribed:

$$w = \hat{w}_1 \cos\frac{2\pi t}{T_1} \sin\frac{2\pi z}{\lambda_1} + \hat{w}_2 \cos\left(\frac{2\pi t}{T_2} + \phi_{w2}\right) \sin\frac{2\pi z}{\lambda_2} \tag{13}$$

$$v = \hat{v}_1 \cos\left(\frac{2\pi t}{T_1} + \phi_{v1}\right) \cos\frac{2\pi z}{\lambda_1} + \hat{v}_2 \cos\left(\frac{2\pi t}{T_2} + \phi_{v2}\right) \cos\frac{2\pi z}{\lambda_2} \tag{14}$$

$$u = \hat{u}_1 \cos\left(\frac{2\pi t}{T_1} + \phi_{u1}\right) \cos\frac{2\pi z}{\lambda_1} + \hat{u}_2 \cos\left(\frac{2\pi t}{T_2} + \phi_{w2}\right) \cos\frac{2\pi z}{\lambda_2} \tag{15}$$

with $U = \overline{U}(y_0) + u$, where u, v, w are the fluctuating components of the velocity at $y = y_0$ that are associated with the coherent flow and $\overline{U}(y_0)$ is the average streamwise velocity at the same location. The λ_1 components are associated with the $\lambda_1^+ = 100$ eddies, while the λ_2 components reflect contributions from larger scale outer flow eddies.

Finite-difference methods are used to solve Eqs. 9–12. The computations are continued for long enough times for a station-

ary state to be reached (usually about three cycles). A statistical analysis of the calculated results was carried out for the subsequent cycles. This involved taking an average in time over a period T_2 and an average in the z direction over a length λ_2 for a fixed distance, y, from the wall. The mesh sizes and the time intervals were changed to check the accuracy of the computed results. Details regarding the numerical methods may be found in theses by Nikolaides (1984), Finnicum (1986), and Lyons (1985).

Selection of boundary conditions

The parameters in Eqs. 13, 14, and 15 were selected by Nikolaides so as to be consistent with presently available turbulence measurements at $y^+ = 40$. These are:

Parameter	y_0^+	λ_1^+	λ_2^+	T_1^+	T_2^+
Value	40	100	400	100	400

Parameter	E_{u1}	E_{v1}	E_{w1}	ϕ_{u1}	ϕ_{u2}	ϕ_{v1}	ϕ_{v2}	ϕ_{w2}
Value	0.15	0.75	0.40	216	194.4	36	90	270

Here E represents the fraction of the energy of a velocity component at $y_0^+ = 40$ contained in the λ_1^+ eddies. Thus $E_{w1} = \hat{w}_1^2/(\hat{w}_1^2 + \hat{w}_2^2)$. The rationale behind the selection of these parameters is presented in great detail in the thesis by Nikolaides.

All presently available measurements suggest that the $\lambda_1^+ = 100$ eddies would roughly correspond to the smallest eddies present at $y^+ = 40$. The influence of all larger size eddies is represented by the $\lambda_2^+ = 400$ component. It is to be noted that the λ_1^+ stress producing eddies are assumed to contain 15% of the u energy, 40% of the w energy, and 75% of the v energy.

Frequency spectra of the velocity fluctuations in the viscous sublayer (Bakewell and Lumley, 1967) and of the wall shear stress fluctuations (Hanratty et al., 1977) indicate a median frequency of $n^+ \simeq 0.01$. This suggests $T_1^+ \simeq 100$. This selection is also consistent with the assumption that at distances away from the wall, where viscosity is not very important, the transient terms must be the same order as the convective terms in order that the eddies be dynamically important. Thus, since velocities scale with u^*,

$$\frac{\partial w}{\partial t} \sim w\frac{\partial w}{\partial z} \Rightarrow \frac{u^*}{T} \sim \frac{u^{*2}}{\lambda} \Rightarrow T^+ \sim \lambda^+ \qquad (16)$$

This latter reasoning is used to set $T_2^+ = \lambda_2^+ = 400$.

The phase angles (ϕ_{v1}, $\phi_{v2} - \phi_{w2}$) determine the percent of the time the eddy pattern is open or closed at $y_0^+ = 40$. Thus ($\phi_{v2} - \phi_{w2}$) was set equal to $-180°$ so that the streamlines of the large λ_2 eddies are open all the time, Figure 1b. Phase angle ϕ_{v1} was set equal to 36° so that streamlines of the λ_1 eddies were closed for $0 < y^+ < 40$ and open for $0 < y^+ < 20$ most of the time, Figure 1a, to be consistent with measurements of Kreplin and Eckelman (1979) and of Nikolaides et al (1983). Phases $\phi_{u1} - \phi_{v1}$ and $\phi_{u2} - \phi_{v2}$ were chosen so as to correctly specify the Reynolds stress at $y_0^+ = 40$.

The value of $\bar{U}_0^+$ was adjusted so that $\bar{U}^+ = y^+$ for $y \to 0$.

Calculated Results for $\lambda_1^+ = 100$

Figures 2–6 give a comparison between measurements and the calculated profiles of the mean velocity, the Reynolds stress, and the turbulence intensity. Good agreement is noted for the mean velocity and the Reynolds stress.

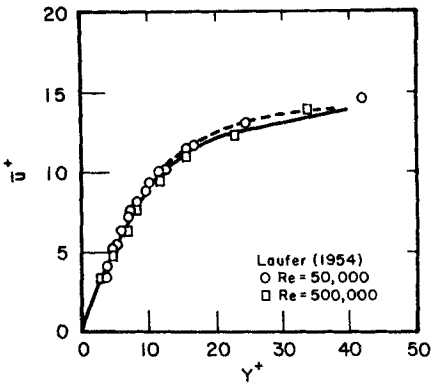

Figure 2. Mean streamwise velocity profiles, $y_0^+ = 40$.
— Using a double harmonic
--- Using a single harmonic

The calculated intensities of the x component, $\overline{u^2}$, are somewhat higher than the measurements but show the maximum at $y^+ = 12$ found in the measurements. The calculated magnitude and location of this maximum is roughly the same if the x component of the velocity fluctuations is assumed to be zero at y_0. The model, therefore, indicates that the large streamwise velocity fluctuations close to the wall are the result of a creation of turbulence by the secondary flow. The calculated flatness, $\overline{u^4}$, and skewness, $\overline{u^3}$, of the streamwise velocity fluctuations also show good agreement with measurements.

The calculated profile of the intensity of the normal velocity fluctuations, $\overline{v^2}$, is in good agreement with measurements, particularly since there is evidence to suggest that probe interference errors could cause the measurements to be high (Finnicum and Hanratty, 1985). The agreement between calculated $\overline{w^2}$ profiles and the measurements of Laufer (1954) is good. The calculations of $\overline{w^2}$ show an interesting inflection at $y^+ < 20$. The measurements are not accurate enough to confirm the existence of such an inflection.

A close examination of the calculations in the neighborhood y_0 reveals rapid changes in the turbulence that are nonphysical. This is shown by the sudden drop in the Reynolds stress and sudden increases in the calculated flatnesses and skewnesses. However, it is in stronger evidence in the calculated streamwise vorticity, shown in Figure 7.

These rapid changes at the outer edge of the computational

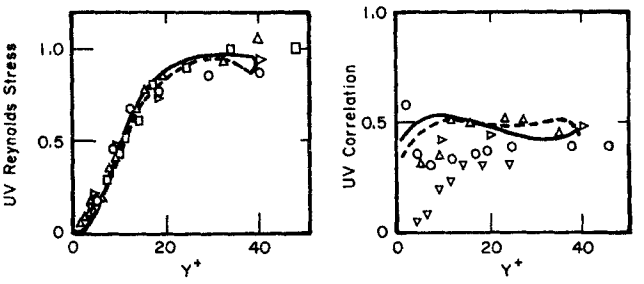

Figure 3. Reynolds stress and $-\overline{uv}/\overline{u'v'}$ correlation, $y_0^+ = 40$.
— Using a double harmonic; --- Using a single harmonic

(Left)		(Right)	
▷	Laufer (1954)	▷	Laufer (1954)
△□	Gupta et al. (1971)	∩	Kim et al. (1971)
○	Schildnecht et al. (1979)	▽	Kutateladze et al. (1977)
		○	Eckelmann (1974)

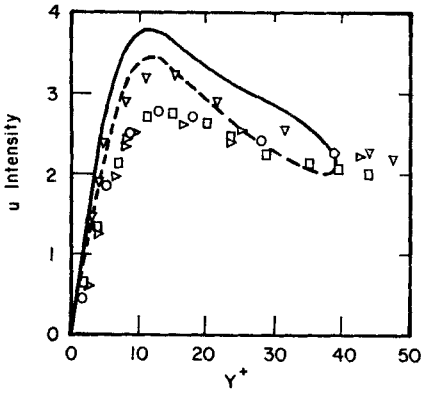

Figure 4. Intensity of streamwise velocity fluctuations, $y_0^+ = 40$.

— Using a double harmonic; --- Using a single harmonic
▽ Clark (1968)
▷ Laufer (1954)
○ Schildnecht et al. (1979)

domain suggest that the form of the outer boundary conditions is too restrictive and that this causes the existence of a viscous region of high vorticity close to y_0. The specification of asymptotic conditions or of derivatives at the outer boundary could, possibly, avoid this difficulty.

Fortunately, this error affects calculations only over the outer 10–20% of the viscous wall region. Consequently, discussions of energy balances presented in the following sectoins will disregard calculations for the region $0.85\, y_0^+ < y^+ < 1.0\, y_0^+$.

Calculated Effect of λ_1^+

Calculations of effect of λ_1^+ using two harmonics

In order to use this model to calculate the effect of changes of λ_1^+ it is necessary to determine how the specified boundary conditions discussed previously should be changed if λ_1^+ is changed.

If it is assumed that y_0^+ is in a log layer, then Eq. 5 suggests that $(\overline{w^2})^{1/2}/u^*$, $(\overline{v^2})^{1/2}/u^*$, and $(\overline{u^2})^{1/2}/u^*$ should remain unchanged. Experimental measurements show that $\lambda_1^+ = 100$ for $y_0^+ = 40$ so that Eq. 8 gives

$$\lambda_1^{+2} = 250\, y_0^+ \tag{16}$$

Equation 8 therefore suggests that y_0^+ should be increased with increases in λ_1^+. Furthermore Eq. 16 indicates that T_1^+ should be increased with increases in λ_1^+ so that $T_1^+ = \lambda_1^+$.

No theoretical guidance was available for selecting λ_2^+ or for

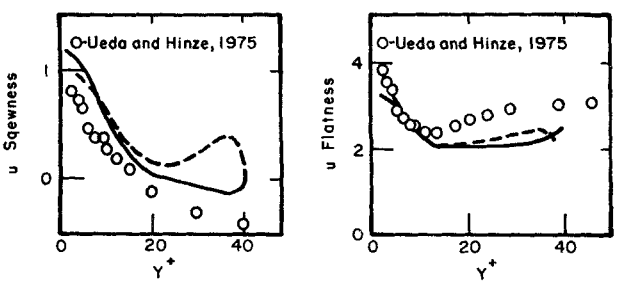

Figure 5. Skewness and flatness of streamwise velocity fluctuations for single and double harmonic runs.

Upper boundary at $y_0^+ = 40$

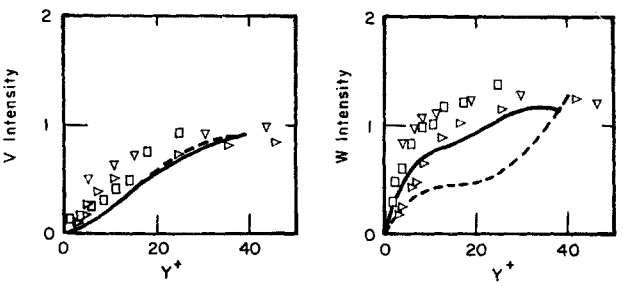

Figure 6. Intensities of normal and spanwise components of velocity, $y_0^+ = 40$.

— Using a double harmonic; --- Using a single harmonic
▽ Clark (1968)
▷ Laufer (1954)
□ Kutateladze et al. (1977)

selecting the phase angles. Therefore, the phase angles and λ_2^+ were kept constant for the calculations with different λ_1^+.

Calculations of the effect of λ_1^+ using one harmonic

Because of the uncertainty of how to specify changes of the outer flow, λ_2^+, eddies with changes in λ_1^+, calculations were also carried out for the case of $\lambda_2^+ = \infty$ in order to see how sensitive the results are to the specification of λ_2^+.

Nikolaides (1984) showed that the velocity field could be represented in the region $0 < y^+ < 40$ if the parameters in Eqs. 13, 14, and 15 are given the following values:

Parameter	y_0^+	λ_1^+	T_1^+	λ_2^+	T_{u2}^+
Value	40	100	100	∞	400

Parameter	E_{u1}	E_{v1}	E_{w1}	ϕ_{u1}	ϕ_{v1}	ϕ_{u2}
Value	0.15	1.00	1.00	25.2	72	150

It is to be noted that the outer flow eddies are assumed to be homogeneous in the z and y directions ($\hat{w}_2 = \hat{v}_2 = 0$) and to have an infinite wavelength in the x direction. Thus,

$$u = \hat{u}_1 \cos\left(\frac{2\pi t}{T_1} + \phi_{u1}\right) + \hat{u}_2 \cos\left(\frac{2\pi t}{T_2} + \phi_{u2}\right) \tag{17}$$

For calculations with $\lambda_1^+ \neq 100$ the values of y_0^+, T_1^+, and T_2^+ were changed so that $T_1^+ = \lambda_1^+$, that $T_2^+ \approx 400$, and that Eq. 16 is satisfied.

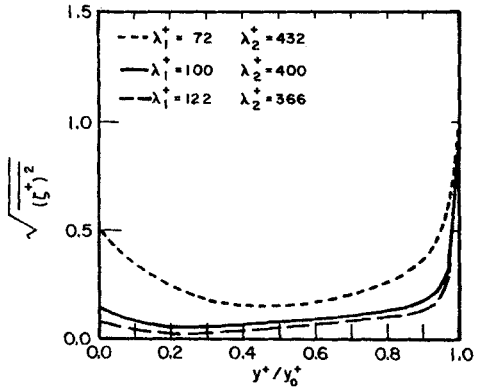

Figure 7. Vorticity intensity for two-harmonic runs.

A comparison of calculations using the one- and two-wavelength models for $\lambda_1^+ = 100$ is given in Figures 2–6.

Results on the effect of λ_1^+

The calculated effect of a change of λ_1^+ on the average velocity profile is given in Figure 8 where, it is to be noted, the abscissa is normalized with y_0^+. It is seen that an increase in λ_1^+ causes an increase of $\overline{U}^+$ at $y^+ = y_0^+$, or an increase in the volumetric flow for a given τ_w. Thus, the calculation is consistent with the experimental finding that drag reduction is associated with an increase in λ_1^+.

The most important result obtained from the calculations is the effect of λ_1^+ on the balance of turbulent kinetic energy, $q^2 = \frac{1}{2}(u^2 + v^2 + w^2)$. For the model flow being considered,

$$0 = \underbrace{-\overline{uv}\frac{d\overline{U}}{dy}}_{\text{I}} \underbrace{-\frac{d\overline{vq^2}}{dy}}_{\text{II}} \underbrace{-\frac{1}{\rho}\frac{d\overline{vp}}{dy}}_{\text{III}} \underbrace{+\nu\frac{d^2\overline{q^2}}{dy^2}}_{\text{IV}} \underbrace{-\nu\left(\overline{\frac{du_i}{dx_j}}\right)^2}_{\text{V}} \qquad (18)$$

Term I, which is always positive, represents the production of turbulent energy. It will be designated by the symbol P. Terms II, III, and IV respectively represent the transfer of kinetic energy by the turbulent velocity, the transfer of pressure energy by the turbulent velocity, and the transfer of kinetic energy by molecular viscosity. Term V is always negative and represents the dissipation of turbulence, designated by the symbol $-\epsilon$.

If Eq. 18 is integrated from y_0^+ to the outer boundary of the turbulent region, δ,

$$(\overline{vq^2} + \overline{vp})_{\text{at}y_0} - \nu\left(\frac{d\overline{q^2}}{dy}\right)_{\text{at}y_0} = -\int_{y_0}^{\delta}(P - \epsilon)\,dy \qquad (19)$$

In the log region $P \cong \epsilon$, and term IV is small. Thus the sum of terms II and III is zero and $(\overline{vq^2} + \overline{vp})$ is a constant. Beyond the log region $P < \epsilon$, so there is a net dissipation of energy in the region outside the viscous wall region ($y^+ > y_0^+$). This energy is supplied by a diffusion of energy out of the viscous wall region, represented by the lefthand side of Eq. 19, if the turbulence is stationary.

The main goal of this paper is to show how the lefthand side of Eq. 19 varies with λ_1^+. Since the calculations are least accurate close to y_0^+, this term was evaluated by considering the integral of Eq. 18 from 0 to y_0^+.

$$\int_0^{y_0}(P - \epsilon)\,dy = (\overline{vq^2} - \overline{vp})_{\text{at}y_0} - \nu\left(\frac{d\overline{q^2}}{dy}\right)_{\text{at}y_0} \qquad (20)$$

since $(d\overline{q^2}/dy)_{\text{at}0} = 0$.

The energy balance terms in Eq. 18 calculated for $\lambda_1^+ = 100$ are shown in Figure 9. Close to the wall the energy dissipation (term V) is a maximum and the production (term I) is small. Energy is supplied to $0 < y^+ < 0.1\ y_0^+$ by a viscous diffusion of energy (term IV) produced at $y^+ > 0.1\ y_0^+$. At the outer part of the viscous wall region the production of turbulent energy (term I) is approximately equal to the dissipation (term V). The important property to be noted is that both the production and the dissipation are quite large in the viscous wall region and that the flow of energy out is represented by the integral of the difference of two large numbers (the lefthand side of Eq. 20).

Values of $\int_0^{y_0^+}(P - \epsilon)\,dy^+$ calculated for different values of λ_1^+ are shown in Figure 10. It is noted that for the calculations with two harmonics this integral is positive for $\lambda_1^+ = 100$ and for $\lambda_1^+ = 122$, and is negative for $\lambda_1^+ = 72$. This calculation would suggest that $\lambda_1^+ = 72$ would give an impossible stationary situation since it requires a diffusion of turbulent energy into the viscous wall region.

Of interest is the large change in the net production of turbulent energy with an increase of λ_1^+ from 72 to 100. Laufer's (1954) pipe flow measurements indicate a dimensionless net dissipation of turbulent energy of 0.29 in the core region. Using a linear interpolation, a value of $\lambda_1^+ = 93$ is obtained as needed to satisfy the balance of mechanical energy.

Calculations using a single eddy representation of the viscous wall region are also given in Figure 10. These show the same qualitative behavior as the model with two harmonics and give a value of $\lambda_1^+ = 114$ as needed to provide a net production of 0.29.

Both estimates for λ_1^+ are close to the observed characteristic scale for the viscous wall region of 100 wall units.

Summary

The model developed by Nikolaides is strongly similar to that proposed by Townsend (1976, pp. 150–156). A consequence of the established law of the wall is that the dissipation length, ℓ,

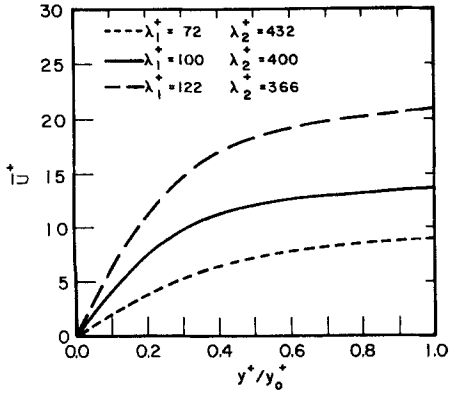

Figure 8. Mean velocity profiles for two-harmonic runs.

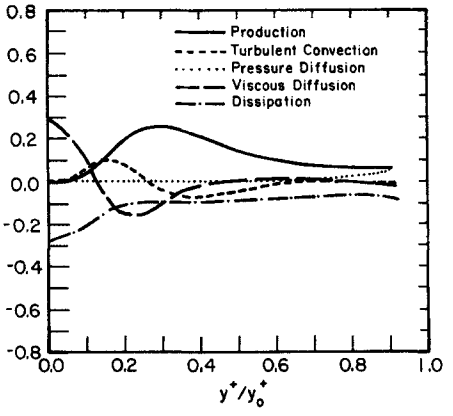

Figure 9. Turbulent kinetic energy balance using two-harmonic model.
$\lambda_1^+ = 100$; $\lambda_2^+ = 400$

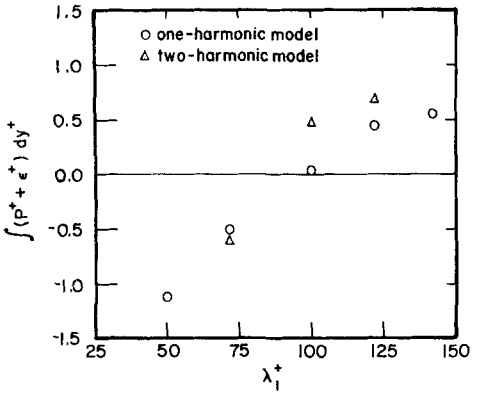

Figure 10. Net production of turbulent kinetic energy by viscous wall region for various λ_1^+.

varies linearly with distance from the wall in the log layer. Townsend argues that this implies that the velocity fields of the main eddies (regarded by him as persistent, organized flow patterns) extend to the wall and, "in a sense, are attached to the wall." He therefore suggests that the observed characteristics of the flow in the constant stress region can be considered to be made up from inputs of attached eddies of a wide range of sizes, for which the contributions to the Reynolds stress is concentrated in the general neighborhood of the distance from the wall of their center.

In the context of Townsend's picture of an equilibrium constant stress layer, the $\lambda^+ \equiv 100$ eddy modeled by Nikolaides is the most important one in the viscous wall region $0 < y^+ < y_0^+ = 40$ and is the smallest one of any importance in the log layer. It completely dominates the flow close to the wall ($0 < y^+ < 15$) and is a weak contributor over most of the log layer. Therefore, in order to extend the calculations from $y^+ = 15$ out to the inner edge of the log layer larger eddies must also be considered. This is done in a simplified manner by representing the interaction between the log layer and the viscous wall layer with only two scales, $\lambda_1^+ = 100$, $\lambda_2^+ = 400$.

The calculations of Nikolaides show that the $\lambda_1^+ = 100$ control the production of turbulence in the viscous wall region. These disturbances bring high-momentum fluid toward the wall, exchange momentum to the wall to create velocity-deficient fluid, and transport this velocity-deficient fluid away from the wall.

By this process, the wall layer eddies convert the mean flow energy, transported to the viscous wall region, into large streamwise velocity fluctuations. This is manifested by the observed maximum in $\overline{u^2}$ at $y^+ = 12$ and the finding that the calculated variation of $\overline{u^2}$ with y^+ close to the wall is independent of the streamwise velocity fluctuations superimposed at y_0^+. The conversion of these streamwise velocity fluctuations into normal and spanwise fluctuations occurs mainly beyond $y_0^+ = 40$, through a correlation between fluctuations in the pressure and velocity derivatives in the flow direction. This type of picture does not imply an absence of spanwise and normal velocity fluctuations at $y_0^+ = 40$ but only that they are created at large y^+ and convected to y_0^+, where they cause the flow-oriented structures at the wall.

The interaction between the inner and outer flow outlined above determines the characteristic length λ_1^+. This paper suggests that a consideration of the balance of mechanical energy could provide an understanding of this interaction. According to Townsend, mean flow energy is transferred to the wall region where it is converted into turbulent energy. The production of turbulent energy is quite large in the viscous wall region, but so is the dissipation of energy. It is the difference of these two large numbers that supplies the energy necessary to fuel the dissipative processes in the core.

The most important result of the calculations is that in the neighborhood of $\lambda_1^+ = 100$, the net amount of turbulent energy produced in the viscous wall region is very sensitive to changes in λ_1^+. This is not surprising if one considers that the total production of turbulent energy in the viscous wall region is 3.1 times the total energy dissipated in the outer flow. The amount of energy dissipated in the viscous wall region is of the same order as the amount produced, and it increases with decreasing λ_1^+. This explains why the calculations show that the viscous wall region changes its role from a net producer to a net consumer of turbulent energy as λ_1^+ decreases.

These types of considerations then suggest the following type feedback between the inner and outer flows: If λ_1 is proportional to the Taylor microscale, as suggested by Nikolaides, then from Eq. 7 one would expect λ_1 to decrease if the level of dissipation in the core increases. The calculations suggest that this decrease would cause a decrease in the net production of turbulent energy in the viscous wall region which, in turn, would lower the energy available for dissipation in the core.

Acknowledgment

This work has received support from the Office of Naval Research under Project NR 657-728, and from the Shell Companies Foundation.

Notation

C_i = constants, Eqs. 3, 4, 8, 9, 11
E = fraction of the energy of a velocity component at y_0 that is contained in the λ_1 eddies
ℓ = characteristic length of large eddies
N_0 = frequency of zero crossings per unit length
p = pressure
P = production of turbulent energy
$q = (\overline{u^2} + \overline{v^2} + \overline{w^2})^{1/2}$
Re = Reynolds number
t = time
T = period
T_B = bursting period
u = fluctuating streamwise velocity
u^* = friction velocity $= (\tau_w/\rho)^{1/2}$
U = streamwise velocity
V = velocity normal to wall
v = fluctuating velocity component normal to wall
W = velocity component in the spanwise direction
w = fluctuating spanwise velocity component
x = coordinate in the flow direction
y = coordinate to wall
z = coordinate in spanwise direction

Greek letters

ϵ = rate of dissipation of turbulent energy
κ = Von Karman constant = 0.41
ϕ_i = phase of velocity component i
λ_i = wavelength of component i
λ = streak spacing
λ_T = Taylor microscale
Λ = zero crossing scale
μ = molecular viscosity
ρ = density of fluid
τ_w = wall shear stress

Superscripts

+ = nondimensional with friction velocity u^* and kinematic viscosity ν
− = time average
|ˆ| = amplitude

Subscripts

0 = quantity located at outer edge of viscous wall region
w = evaluated at wall
1 = quantity associated with inner eddies
2 = quantity associated with outer eddies

Literature Cited

Bakewell, H. P., and J. L. Lumley, "Viscous Sublayer and Adjacent Wall Region in Turbulent Pipe Flow," *Phys. Fluids*, **10**, 1880 (1967).

Barlow, R. S., and J. P. Johnston, "Structure of Turbulent Boundary Layers on a Concave Surface," Rept. MD-47, Dept. Mech. Eng., Stanford Univ. (1985).

Bradshaw, P., *Turbulence Topics in Applied Physics*, **12**, Springer, Berlin (1976).

Clark, J. A., "A Study of Incompressible Turbulent Boundary Layers in Channel Flow," *J. Basic Eng.*, **90**, 455 (1968).

Chapman, D. R., and G. D. Kuhn, "Two-Component Navier-Stokes Computational Model of Viscous Sublayer Turbulence," AIAA Paper 81-1024, *Proc. AIAA 5th CFD Conf.*, Palo Alto (1981).

Corino, E. R., and R. S. Brodkey, "A Visual Investigation of the Wall Region in Turbulent Flow," *J. Fluid Mech.*, **37**, 1 (1969).

Corrsin, S., *Symp. on Naval Hydrodynamics*, Pub. No. 515, Nat. Acad. of Sci./Nat. Res. Council, Washington DC, 373 (1956).

Eckelman, L. D., G. Fortuna, and T. J. Hanratty, "Drag Reduction and the Wavelength of Flow-Oriented Wall Eddies," *Nature*, **236**(67), 94 (1972).

Eckelmann, H., "The Structure of the Viscous Sublayer and the Adjacent Wall Region in a Turbulent Channel Flow," *J. Fluid Mech.*, **65**, 439 (1974).

Finnicum, D. S., "Pressure Gradient Effects in the Viscous Wall Region of a Turbulent Flow," Ph.D. thesis, Univ. Illinois, Urbana (1986).

Finnicum, D. S., and T. J. Hanratty, "Turbulent Normal Velocity Fluctuations Close to a Wall," *Phys. Fluids*, **28**, 1654 (1985).

Fortuna, G., and T. J. Hanratty, "The Influence of Drag-Reducing Polymers on Turbulence in the Viscous Sublayer," *J. Fluid Mech.*, **53**, 575 (1972).

Grant, H. L., "The Large Eddies of Turbulent Motion," *J. Fluid Mech.*, **4**, 149 (1958).

Gupta, A. K., J. Laufer, and R. E. Kaplan, "Spatial Structure in the Viscous Sublayer," *J. Fluid Mech.*, **50**, 493 (1971).

Hanratty, T. J., L. G. Chorn, and D. T. Hatziavramidis, "Turbulent Fluctuations in the Viscous Wall Region for Newtonian and Drag-Reducing Fluids," *Phys. Fluids*, **20**, S112 (1977).

Hatziavramidis, D. T., and T. J. Hanratty, "The Representation of the Viscous Wall Region by a Regular Eddy Pattern," *J. Fluid Mech.*, **95**, 655 (1979).

Hinze, J. O., *Turbulence*, 2nd ed., McGraw-Hill, New York (1975).

Kim, H. T., S. J. Kline, and W. C. Reynolds, "The Production of Turbulence Near a Smooth Wall in a Turbulent Boundary Layer," *J. Fluid Mech.*, **50**, 133 (1971).

Kline, S. J., and P. W. Runstadler, "Some Preliminary Results of Visual Studies of the Flow Model of the Wall Layers of the Turbulent Boundary Layer," *J. Appl. Mech.*, **2**, 166 (1959).

Kline, S. J., W. C. Reynolds, F. A. Schraub, and P. W. Runstadler, "The Structure of Turbulent Boundary Layers," *J. Fluid Mech.*, **30**, 741 (1967).

Kreplin, H. P., and H. Eckelman, "Propagation of Perturbations in the Viscous Sublayer and Adjacent Wall Region," *J. Fluid Mech.*, **95**, 305 (1979).

Kutateladze, S. S., E. M. Khabakhpasheva, V. V. Orlov, B. V. Pereplitsa, and E. S. Mikhailova, "Experimental Investigation of the Structure of Near-Wall Turbulence and Viscous Sublayer," *Proc. Symp. Turbulent Shear Flow*, Penn State Univ., **I**, Paper No. 17, 13 (1977).

Laufer, J. "The Structure of Turbulence in Fully Developed Pipe Flow," NACA TN 1174 (1954).

Lee, M. K., L. D. Eckelman, and T. J. Hanratty, "Identification of Turbulent Wall Eddies Through the Phase Relation of the Components of the Fluctuating Velocity Gradient," *J. Fluid Mech.*, **66**, 17 (1974).

Lyons, S. L., "Computer Experiments on the Coherent Structures in the Viscous Wall Region of a Turbulent Flow," M.S. Thesis, Univ. Illinois, Urbana (1985).

Morrison, W. R. B., and R. E. Kronauer, "Structural Similarity for Fully Developed Turbulence in Smooth Tubes," *J. Fluid Mech.*, **39**, 117 (1969).

Nikolaides, C., "A Study of the Coherent Structures in the Viscous Wall Region of a Turbulent Flow," Ph.D. Thesis, Univ. Illionis, Urbana (1984).

Nikolaides, C., K. K. Lau, and T. J. Hanratty, "A Study of the Spanwise Structure of Coherent Eddies in the Viscous Wall Region," *J. Fluid Mech.*, **130**, 91 (1983).

Rice, S. O., *Selected Papers on Noise and Stochastic Processes*, N. Wax, eds., Dover, New York (1954).

Schildnecht, M., J. A. Miller, and G. J. Meier, "The Influence of Suction on the Structure of Turbulence in Fully Developed Pipe Flow," *J. Fluid Mech.*, **90**, 67 (1979).

Tennekes, H., and J. L. Lumley, *A First Course in Turbulence*, 4th ptg. MIT Press, Cambridge, MA (1977).

Townsend, A. A., *The Structure of Turbulent Shear Flow*, 2nd ed., Cambridge Univ. Press (1976).

Tritton, D. J., "Some New Correlation Measurements in a Turbulent Boundary Layer," *J. Fluid Mec.*, **28**, 439 (1967).

Ueda, H., and J. O. Hinze, "Fine-structure Turbulence in the Wall Region of a Turbulent Boundary Layer," *J. Fluid Mech.*, **67**, 125 (1975).

Manuscript received June 11, 1987, and revision received Dec. 17, 1987.